ISSN: 2755-0117

Journal of Oncology Research Reviews & Reports

SCIENTIFIC Research and Community

Research Article

Open Access

Study on the Feasibility of Promoting the Hyperthermia Effect on Superficial Skin Tumors Based on Outdoor Thermal Environment

Yuchen Luo[1], Yong Ding[2], Chenqiu Du[2] and Yong Liu[2*]

[1]Rehabilitation Therapy Department, Second Clinical College of Chongqing Medical University, Chongqing Medical University, Chongqing, China

[2]Joint International Research Laboratory of Green Buildings and Built Environments (Ministry of Education), School of Civil Engineering, Chongqing University, Chongqing, China

ABSTRACT

This study examines whether outdoor thermal conditions can help patients with superficial skin tumors reach the temperatures needed for hyperthermia after hospital discharge. A completely new mathematical model of bio-heat transfer was established to predict temperature changes in skin tissue. The predicted temperature distribution aligns closely with results from the traditional model, indicating that the analytical solution of the new model is meaningful and applicable. Using the tissue temperature profile and the known threshold for hyperthermia, we identified the effective hyperthermia depth for superficial skin tumors. The results of experimental measurements show that in certain outdoor thermal conditions, the skin surface temperature can rise above 39.0C, a level known to suppress tumor growth. Based on these findings, we conclude that some outdoor environments can allow superficial tumors to reach therapeutic temperature levels. This approach may offer patients a more convenient and economical way to support recovery.

***Corresponding author**

Yong Liu, Joint International Research Laboratory of Green Buildings and Built Environments (Ministry of Education), School of Civil Engineering, Chongqing University, Chongqing, China.

Received: March 14, 2026; **Accepted:** March 19, 2026; **Published:** March 28, 2026

Keywords: Skin Tissue, Hyperthermia, Rehabilitation, Superficial Skin Tumor, Outdoor Thermal Environment

Introduction

In recent years, global warming has affected everyone's lives. Long periods of high temperature exposure can affect both physical and physiological functioning. One noticeable change is the steady rise in skin temperature as ambient temperatures increase [1-3]. Junmeng Lyu reported that skin temperature is strongly associated with air temperature and solar radiation and that it responds quickly to environmental variation [4]. Sensitivity also varies across the body: the head and trunk tend to maintain higher skin temperatures and show less fluctuation than the limbs. Wenjie Song noted that the face and hands are the most common sites for skin-temperature measurement due to their higher thermal sensitivity [5]. At the same time, mean skin temperature remains a key physiological indicator in assessing heat exchange between the body and its surroundings [6,7]. Mingxuan Luo Proposed that many studies consider skin temperature the primary physiological marker of health status, with blood pressure and heart rate following behind. Among outdoor thermal factors, solar radiation plays one of the most significant roles in altering skin temperature [8]. Huihui Zhao Found that radiant temperature and its dynamic changes shape people's thermal experiences during clear summer weather [9]. Julian Anders calculated Pearson correlation coefficients between the Universal Thermal Climate Index (UTCI) and influential meteorological variables throughout the diurnal cycle [10]. Because radiation has a strong influence on thermal sensation, the highest daytime correlations were found with mean radiant temperature (MRT, 0.66-0.97) and incoming shortwave radiation (SWR, 0.62-0.92). Outdoor solar radiation also produces more pronounced changes in skin temperature. Overall, skin temperature serves as an indicator of thermal sensation, closely linked to radiation levels in the outdoor environment [11-13].

Based on the above findings, the outdoor thermal environment can raise human skin temperature. This raises two questions: can skin temperature in outdoor conditions reach the threshold required for hyperthermia, and if so, what is the effective hyperthermia depth beneath the skin surface? To address these questions, it is necessary to first outline the principles of hyperthermia.

Tumors pose a significant threat because they reduce quality of life and contribute to premature death [14,15]. Hyperthermia is a therapeutic technique that elevates the temperature of tumor-affected tissue [16,17]. Among treatments that disrupt the homeostasis of tumor cells, hyperthermia has shown promising anti-tumor effects [18-20]. It is also considered environmentally sustainable and generally safe for patients. There are two main types of hyperthermia: thermal ablation, which heats the tumor above 60°C, and mild hyperthermia, which operates between 41-45°C [21]. Thermal ablation targets the tumor core directly, while mild hyperthermia affects a broader region, including surrounding surface tissues. Hyperthermia begins to alter the tumor microenvironment at temperatures as low as 39°C by increasing perfusion and reoxygenation [22-24]. Because mild hyperthermia does not sharply distinguish between tumor and nearby normal tissues both are typically heated to similar levels [25,26]. However,

tumor tissue tends to be 1-3°C warmer than normal tissue [27-29]. Thus, if the tumor reaches the therapeutic range of 39-45°C the adjacent subcutaneous tissue only needs to reach about 38°C from a conservative standpoint [30-32]. Clinically, hyperthermia is often used as an adjuvant treatment to enhance chemotherapy and radiation therapy. These procedures are usually carried out indoors with controlled thermal conditions using radiofrequency, microwave, or ultrasound equipment. A review of prior studies shows that research has focused almost entirely on indoor temperature regulation, with little attention given to outdoor environments. This paper introduces an alternative approach: using outdoor thermal conditions to support hyperthermia for patients with superficial skin tumors after hospital discharge. Drawing on measured data of skin-surface temperature under different outdoor conditions, we show that skin temperature can reach approximately 41°C when air temperature is around 30°C and direct solar radiation is present. These findings suggest that, for patients with superficial skin tumors, outdoor exposure may provide a feasible means of achieving mild hyperthermia.

Based on the principles of hyperthermia and the measured skin-temperature data, it is clear that superficial skin tumors can reach the critical threshold of 39°C under certain outdoor conditions. However, the depth to which this heating effect extends into underlying tissue remains uncertain, making an analysis of subsurface temperature distribution necessary. Much of the existing research on tissue heat transfer relies on the Pennes bio-heat transfer equation. Most studies extend the original model and incorporate additional factors to address specific research needs. Because the classical Pennes equation does not allow for a direct analytical solution, researchers have relied heavily on numerical methods, which often lead to complex solution procedures. Ping Yuan applied a finite-difference method to compute tissue temperature distribution using the Pennes bio-heat transfer equation together with a two-equation porous model, and then used a conjugate-gradient method to estimate the equivalent heat-transfer coefficient for that model [33]. Saqib Mubarak developed a multi-compartment mathematical model of neonatal thermoregulation based on the Pennes equation with appropriate boundary and initial conditions [34]. In related work, three-layer skin models with different thermal properties have been simulated and thermal-wave bio-heat equations have been solved using finite-difference methods [35]. Dual-phase models have also been proposed to address limitations of earlier dual-phase lag formulations that simply modified the classical Pennes equation [36]. Many approaches to solving the Pennes equation rely on numerical methods implemented through specialized computational software [37-39]. Jeantide Said Camilleri used computational simulations in which the Pennes bio-heat equation was applied to model heat exchange within biological tissue [40]. In this work, the tissue thermal-response equation (TRTE) was coupled with the Pennes bio-heat transfer equation (BHTE) to examine the thermal behavior of the tissue, and the BHTE was solved using the finite-volume method (FVM) [41]. Yundong Tang compared four bio-heat equations by analyzing therapeutic temperature distribution and heat-induced tissue damage in a geometric model constructed from computed-tomography images of a tumor [42]. Teerapot Wessapan investigated SAR, fluid flow, and heat transfer in biological tissue under electromagnetic near-field exposure [43]. This coupled model of EM-field propagation, heat transfer, and blood-flow analysis was solved using the finite-element method, and all computational steps were implemented in COMSOL Multiphysics.

The aim of this study is to develop a simpler approach for establishing and solving a bio-heat transfer equation that incorporates blood perfusion, without relying on complex numerical methods. We introduce an analytical solution for a new bio-heat transfer model, which makes the calculation process more straightforward. Using this model, we derive tissue-temperature distributions under several boundary conditions, allowing us to estimate internal tumor temperatures in outdoor thermal environments.

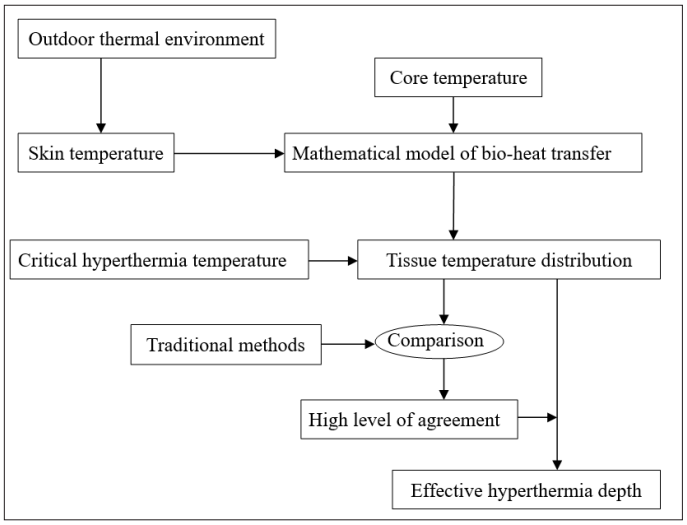

Figure 1: Diagram of the Mathematical Model

Descriptions of the Mathematical Model and its Solution

The Construction Process of the Mathematical Model

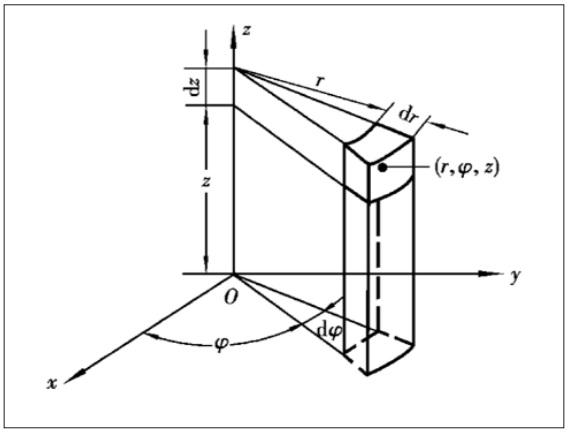

Figure 2: Cylindrical Coordinates Model of the Bio-Heat Transfer [44]

Heat conduction in the r direction, Qr (*W*):

$$Q_r = \left[-k_m \cdot dz \cdot rd\varphi \cdot \frac{\partial T}{\partial r}\right] - \left[-k_m \cdot dz \cdot rd\varphi \cdot \frac{\partial T}{\partial r} + \frac{\partial}{\partial r}(-k_m \cdot dz \cdot rd\varphi \cdot \frac{\partial T}{\partial r}) \cdot dr\right]$$

$$= \frac{\partial}{\partial r}(k_m \cdot r \cdot \frac{\partial T}{\partial r}) \cdot dr \cdot dz \cdot d\varphi$$

k_m-Tissue thermal conductivity, W/(m·K)

Heat conduction in the z direction, Q_z (W):

$$Q_z = \left[-k_m \cdot dr \cdot rd\varphi \cdot \frac{\partial T}{\partial z}\right] - \left[-k_m \cdot dr \cdot rd\varphi \cdot \frac{\partial T}{\partial z} + \frac{\partial}{\partial z}(-k_m \cdot dr \cdot rd\varphi \cdot \frac{\partial T}{\partial z}) \cdot dz\right]$$

$$= \frac{\partial}{\partial z}(k_m \cdot \frac{\partial T}{\partial z}) \cdot dr \cdot rd\varphi \cdot dz$$

Heat conduction in φ direction, Q_φ(W):

$$Q_\varphi = \left[-k_m \cdot dr \cdot dz \cdot \frac{\partial T}{\partial (r\varphi)}\right]$$

$$- \left[-k_m \cdot dr \cdot dz \cdot \frac{\partial T}{\partial (r\varphi)} + \frac{\partial}{\partial (r\varphi)}(-k_m \cdot dr \cdot dz \cdot \frac{\partial T}{\partial (r\varphi)})d(r\varphi)\right]$$

$$= \frac{\partial}{\partial (r\varphi)}(k_m \cdot dr \cdot dz \cdot \frac{\partial T}{\partial (r\varphi)})d(r\varphi)$$

$$= \frac{\partial}{\partial \varphi}(k_m \cdot \frac{\partial T}{\partial \varphi}) \cdot dr \cdot dz \cdot d\varphi \cdot \frac{1}{r}$$

Heat produced by tissue, Q_t (*W*):

$Q_t = Q_m \cdot dr \cdot rd\varphi \cdot dz$

Q_m-Metabolic heat-production rate, (W/m^3)

Energy variation for the elemental volume, Q_e (W):

$$Q_e = \frac{\partial(\rho \cdot dr \cdot dz \cdot rd\varphi \cdot c \cdot T)}{\partial \tau} d\tau$$

$$= \frac{\partial T}{\partial \tau} \cdot \rho \cdot (dr \cdot dz \cdot rd\varphi) \cdot c \cdot d\tau$$

$$= \frac{\partial T}{\partial \tau} \cdot \rho \cdot (dr \cdot dz \cdot rd\varphi) \cdot c$$

Here, dτ=1
c-Specific heat of tissue, (J/Kg·K);

Convective heat transfer between arterial blood and tissue, Q_c (*W*):

$Q_c = W_b C_b[T_a - (r \cdot n + b)] \cdot (dr \cdot dz \cdot rd\varphi)$

(r·n+b)-Venous blood temperature; the parameters n and b are determined by the skin temperature and core temperature.
W_b-Blood perfusion rate, ($kg/m^3 \cdot s$);
C_b-Specific heat of blood, (J/Kg·K);
T_a-Artery blood temperature, (℃);

The Energy Balance Equation for the Elemental Volume:

$$Q_e = \mathrm{Q_r} + \mathrm{Q_z} + \mathrm{Q_\varphi} + \mathrm{Q_t} + Q_c \ (1)$$

$$\frac{\partial \mathrm{T}}{\partial \tau} \cdot \rho \cdot (\mathrm{dr} \cdot \mathrm{dz} \cdot \mathrm{rd}\varphi) \cdot \mathrm{c} = \frac{\partial}{\partial \mathrm{r}}(k_m \cdot \mathrm{r} \cdot \frac{\partial \mathrm{T}}{\partial \mathrm{r}})\mathrm{dr} \cdot \mathrm{dz} \cdot \mathrm{d}\varphi + \frac{\partial}{\partial \mathrm{z}}(k_m \cdot \frac{\partial \mathrm{T}}{\partial \mathrm{z}})\mathrm{dr} \cdot \mathrm{rd}\varphi \cdot \mathrm{dz} + \frac{\partial}{\partial \varphi}(k_m \cdot \frac{\partial \mathrm{T}}{\partial \varphi})\mathrm{dr} \cdot \mathrm{dz} \cdot \mathrm{d}\varphi \cdot \frac{1}{\mathrm{r}} + Q_m \cdot \mathrm{dr} \cdot \mathrm{rd}\varphi \cdot \mathrm{dz} + W_b C_b[T_a - (\mathrm{r} \cdot \mathrm{n} + \mathrm{b})] \cdot (\mathrm{dr} \cdot \mathrm{dz} \cdot \mathrm{rd}\varphi)$$

$$\frac{\partial \mathrm{T}}{\partial \tau} \cdot \rho \cdot \mathrm{c} = \frac{\partial}{\partial \mathrm{r}}\left(k_m \cdot \mathrm{r} \cdot \frac{\partial \mathrm{T}}{\partial \mathrm{r}}\right) \cdot \frac{1}{\mathrm{r}} + \frac{\partial}{\partial \mathrm{z}}\left(k_m \cdot \frac{\partial \mathrm{T}}{\partial \mathrm{z}}\right) + \frac{\partial}{\partial \varphi}\left(k_m \cdot \frac{\partial \mathrm{T}}{\partial \varphi}\right) \cdot \frac{1}{\mathrm{r}^2} + Q_m + W_b C_b[T_a - (\mathrm{r} \cdot \mathrm{n} + \mathrm{b})] \ (2)$$

In this paper, heat conduction in the φ and z direction is neglected, and equation (2) is therefore reduced to:

$$\frac{\partial \mathrm{T}}{\partial \tau} \cdot \rho \cdot \mathrm{c} = \frac{\partial}{\partial \mathrm{r}}(k_m \cdot \mathrm{r} \cdot \frac{\partial \mathrm{T}}{\partial \mathrm{r}}) \cdot \frac{1}{\mathrm{r}} + Q_m + W_b C_b[T_a - (\mathrm{r} \cdot \mathrm{n} + \mathrm{b})] \ (3)$$

Assuming steady-state heat transfer, equation (3) is further simplified to equation (4):

$$\frac{1}{r}\frac{d}{dr}\left(r \cdot k_m \cdot \frac{dT}{dr}\right) + W_b C_b(T_a - \mathrm{r} \cdot \mathrm{n} - \mathrm{b}) + Q_m = 0 \ (4)$$

Solution of the Mathematical Model

The steps for solving equation (4) are outlined below:

$$\frac{1}{r}\frac{d}{dr}\left(r \cdot k_m \cdot \frac{dT}{dr}\right) + W_b C_b(T_a - \mathrm{r} \cdot \mathrm{n} - \mathrm{b}) + Q_m = 0$$

$$\frac{1}{r}\frac{d}{dr}\left(r \cdot k_m \cdot \frac{dT}{dr}\right) + W_b C_b(T_a - \mathrm{b}) - n \cdot W_b C_b \cdot \mathrm{r} + Q_m = 0$$

$$\frac{d}{dr}\left(r k_m \frac{dT}{dr}\right) + W_b C_b(T_a - \mathrm{b})r - n \cdot W_b C_b \cdot r^2 + Q_m \cdot r = 0$$

$$\int \frac{d}{dr}\left(r k_m \frac{dT}{dr}\right)\mathrm{dr} = \int (-W_b C_b(T_a - \mathrm{b})r + n \cdot W_b C_b \cdot r^2 - Q_m \cdot r)dr$$

$$r k_m \frac{dT}{dr} + \frac{1}{2} \times W_b C_b(T_a - \mathrm{b})r^2 - \frac{1}{3} \times n \cdot W_b C_b \cdot r^3 + \frac{1}{2} \times Q_m \cdot r^2 = C_1$$

$$k_m \frac{dT}{dr} + \frac{1}{2} \times W_b C_b(T_a - \mathrm{b})r - \frac{1}{3} \times n \cdot W_b C_b \cdot r^2 + \frac{1}{2} \times Q_m \cdot r = \frac{C_1}{r}$$

$$\int \left[k_m \frac{dT}{dr} + \frac{1}{2} \times W_b C_b(T_a - \mathrm{b})r - \frac{1}{3} \times n W_b C_b r^2 + \frac{1}{2} \times Q_m r\right] dr = C_1 \ln r + C_2$$

$$k_m T + \frac{1}{4} \times W_b C_b(T_a - \mathrm{b})r^2 - \frac{1}{9} \times n W_b C_b r^3 + \frac{1}{4} \times Q_m r^2 = C_1 \ln r + C_2$$

$$T = [C_1 \ln r + C_2 - \frac{1}{4} \times W_b C_b(T_a - \mathrm{b})r^2 - \frac{1}{4} \times Q_m r^2 + \frac{1}{9} \times n W_b C_b r^3]/k_m \ (5)$$

Equation (5) represents the final analytical solution for the tissue-temperature distribution.

W_b in the equation (5) is determined by (Martin Seebass, 1999):

$$W_b = 0.45 + 3.55 \exp\left(-\frac{(T_m - 45.0)^2}{12.0}\right) \quad (6)$$

In equation (6), T_m is the arithmetic mean temperature of the skin surface T_s and the core temperature T_b:

$$T_m = \frac{T_s + T_b}{2}$$

Constants C*1* and C*2* in equation (5) are determined using Dirichlet boundary conditions, which depend on T*s* and T*a*.

Validation of the Mathematical Model

To validate the mathematical model proposed in this paper, the calculated tissue-temperature distribution at various depths for breast was compared with results obtained from the Pennes model and its numerical solution [45]. The parameters and boundary conditions needed for the mathematical model are as follows:

k_m=0.22(J/Kg·K); Q_m=400 (W/m^3); W_b C_b=800(W/m^3·K); T_b=36.3°C; T_s=34.5°C; n=-90; b=40.98;

Using these parameters and the analytical expression from equation (5), the tissue-temperature distribution was derived as follows:

$$T = [C_1 \ln r + C_2 + 836r^2 - 8000r^3]/0.22$$

As the tissue depth affected by outdoor thermal environment is around 0.02m, the constants C_1 and C_2 were determined by the following conditions [46]:

When r=0.052m, T_b=36.3°C

$$7.986 = C_1 \ln r + C_2 + 2.261 - 1.125$$

$$6.85 = -2.957C_1 + C_2$$

When r=0.072m, T_s=34.5°C

$$7.59 = C_1 \ln r + C_2 + 4.334 - 2.986$$

$$6.242 = -2.631C_1 + C_2$$

The resulting values of the two constants are:

C_1=-1.865

C_2=1.335

The tissue-temperature distribution obtained from the mathematical model is:

T=3800r^2-36363.636r^3-8.477 ln$r$+6.068

Figure 3 presents the comparison of tissue temperature between the mathematical model and the reference case.

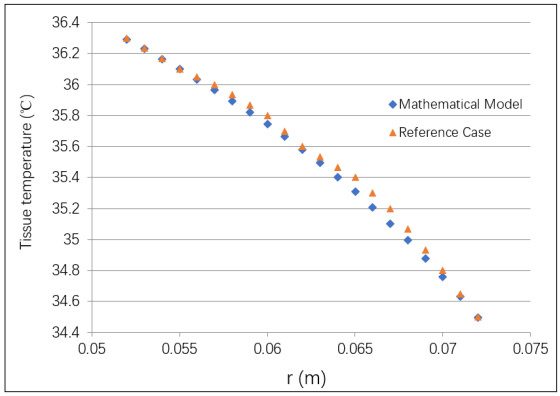

Figure 3: Data Comparison between Mathematical Model and Reference Case

As shown in Fig. 3, the analytical solution produced by the proposed model aligns closely with the temperature distribution obtained from the reference case. This high level of agreement indicates that the analytical solution is meaningful for bio-heat transfer analysis and offers a simpler calculation process compared with traditional numerical methods.

Sensitive Analysis of Skin Surface Temperatures

In this section, the arm is used as the study subject. Several assumed skin-surface temperatures were selected to examine their effects on tissue-temperature distribution. The arm diameter is taken as 0.08 m, and the core temperature is set to 37°C.

The analytical solutions for the different skin temperatures are:

(1) T_s =38°C

$$T = 2.095 \ln r + 45.882 - 2752.636r^2 + 51068.714r^3$$

(2) T_s =39°C

$$T = 3.377 \ln r + 51.464 - 5307.659r^2 + 107846.968r^3$$

(3) T_s =40°C

$$T = 4.632 \ln r + 57.05 - 8376.541r^2 + 176044.318r^3$$

Figure 4 shows the tissue-temperature distribution when the skin-surface temperature is higher than the core temperature.

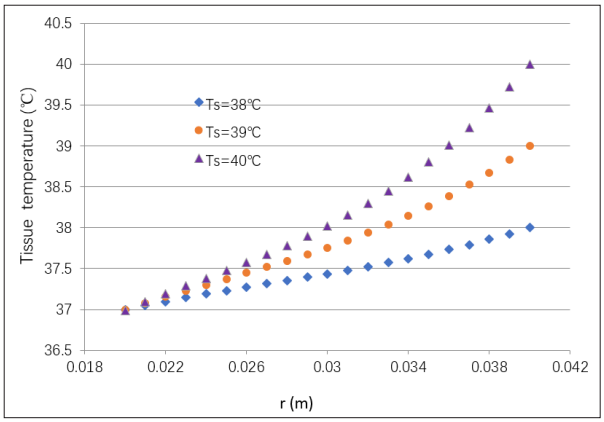

Figure 4: Tissue Temperature Distribution when T_s>T_a

When the skin-surface temperature is lower than the core temperature, the analytical solutions for the tissue-temperature distributions are:

(4) T_s =36°C

$$T = -0.518 \ln r + 34.668 + 1729.355r^2 - 48531.136r^3$$

(5) T_s =35°C

$$T = -1.832 \ln r + 29.059 + 3865.677r^2 - 96004.95r^3$$

(6) T_s =34°C

$$T = -3.136 \ln r + 23.482 + 5997.241r^2 - 143373.032r^3$$

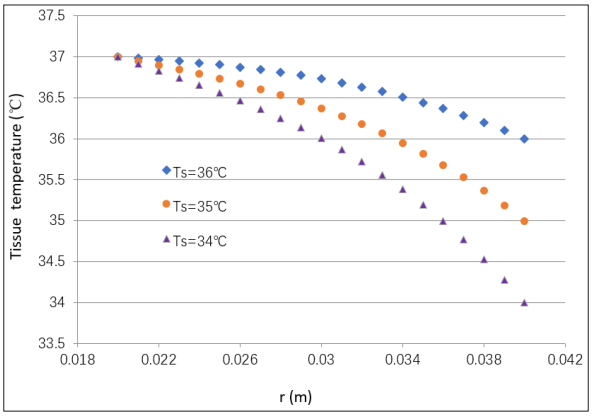

Figure 5: Tissue Temperature Distribution when $T_S<Ta$

Fig.4 and Fig.5 show that when the skin-surface temperature is higher or lower than the core temperature, the corresponding tissue temperatures also rise or fall relative to the core temperature. Based on these temperature distributions, the effective tissue depth that can be reached by hyperthermia can be identified. In Fig. 5, all tissue temperatures remain below the critical hyperthermia threshold, indicating that hyperthermia cannot occur when the skin temperature is lower than the core temperature. This result suggests that outdoor thermal conditions that do not elevate skin temperature above core temperature will be unable to produce a hyperthermia effect.

Results and Discussions

Measurements of Skin Temperature under Outdoor Thermal Environment

The measured parameters include air temperature, skin surface temperature, solar radiation, relative humidity, wind speed, etc. Skin-surface temperature was recorded on the arm once the temperature had stabilized in the outdoor setting. Measurements were taken at 10-second intervals. At the same time, the outdoor environmental parameters were documented to examine how these conditions influence skin-surface temperature.

Three typical scenarios were used in the paper to illustrate how skin-surface temperature responds to different thermal environments. Fig.6 presents the skin-temperature measurements for Case 1 under relatively steady conditions. The outdoor parameters were: air temperature 31.6 °C, solar radiation 684.4 W/m², relative humidity 44%, and wind speed 0.32 m/s. The average measured skin-surface temperature was 40.3 °C. The figure also shows that skin temperature remained fairly stable, reflecting the body's adaptation to the outdoor conditions through sweat evaporation, convection, conduction, and the influence of solar radiation. Fig.7 shows the measurements for Case 2, where the outdoor conditions were air temperature 29.3°C, solar radiation 810.5W/m², relative humidity 41.8%, and wind speed 0.28 m/s. The average skin-surface temperature in this case reached 41.1 °C. Fig.8 presents Case 3, measured under an air temperature of 28.2°C, solar radiation 653.0W/m², relative humidity 69.4%, and wind speed 0.34 m/s. The average skin-surface temperature was 39.5 °C. Across all three cases, skin-temperature trends remained relatively stable once adapted to the outdoor conditions, although the absolute values differed according to each thermal environment. The average skin-surface temperatures from each case were used as boundary conditions in the mathematical model. All outdoor environmental parameters for the three cases are summarized in Table 1.

Table 1: Parameters for the Three Cases

	Average Skin Temperature (℃)	Air Temperature (℃)	Solar Radiation (W/m²)	Wind Speed (m/s)	Relative Humidity (%)
Case 1	40.3	31.6	684.4	0.32	44.2
Case 2	41.1	29.3	810.5	0.28	41.8
Case 3	39.5	28.2	653.0	0.34	69.4

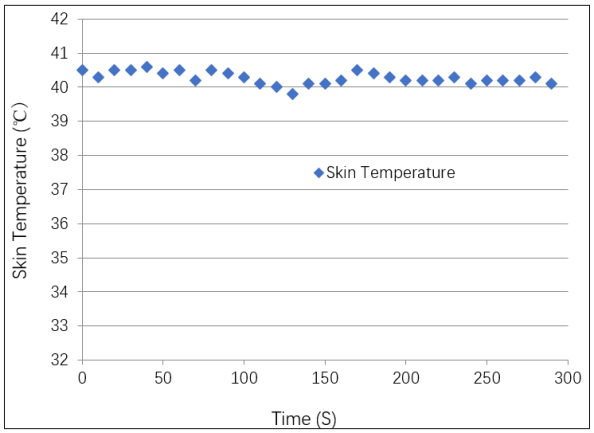

Figure 6: Measured Skin Temperature for Case 1

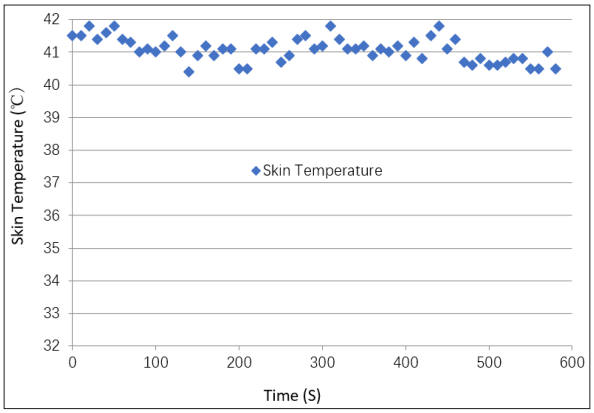

Figure 7: Measured Skin Temperature for Case 2

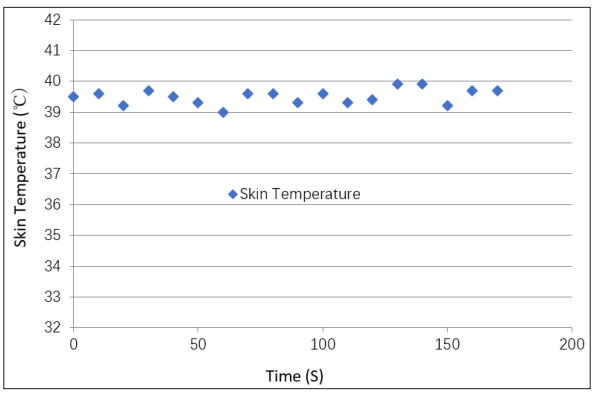

Figure 8: Measured Skin Temperature for Case 3

Determination of the Effective Depth for Hyperthermia

Based on the bio-heat transfer model developed earlier, skin-surface temperature and core temperature were applied as Dirichlet boundary conditions. Using these conditions, the analytical solution of the model was used to determine the temperature distribution within the tissue beneath the skin. The following section outlines the analysis procedure used for the three representative cases.

Case 1

In this case, the skin-surface temperature was 40.3 °C and the core temperature was 37 °C. Using the same procedure described in Section 2.3, the corresponding tissue-temperature profile beneath the skin was obtained:

$$T = 4.995 \ln r + 58.714 - 9451.364r^2 + 199929.25r^3$$

Fig.9 presents the resulting temperature distribution. The commonly referenced threshold for mild hyperthermia is 39°C for tumor tissue. Since tumor temperature is typically 1–3 °C higher than the surrounding normal tissue, a conservative threshold of 38°C was applied to normal tissue. In other words, when normal tissue reaches 38°C, the tumor temperature is expected to be at least 39°C. Based on the above analysis, the effective hyperthermia depth for superficial tumor is 10.6mm in case 1 (see Fig.9).

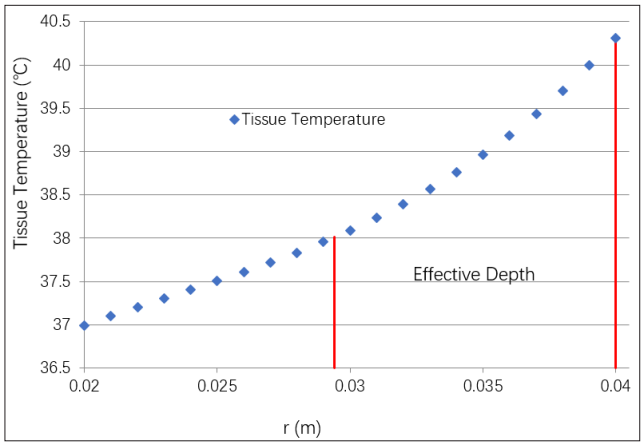

Figure 9: Effective Hyperthermia Depth for Case 1

Case 2

For Case 2, the skin-surface temperature reached 41.1 °C, while the core temperature remained at 37 °C. Using the same approach outlined in Section 2.3, the corresponding tissue-temperature profile beneath the skin was derived:

$$T = 5.927 \ln r + 63.118 - 12861.386r^2 + 275707.605r^3$$

Fig.10 illustrates the resulting temperature distribution. Applying the same criterion for determining the effective hyperthermia depth, the depth at which normal tissue reaches the threshold temperature is 11.3 mm in this case (see Fig. 10).

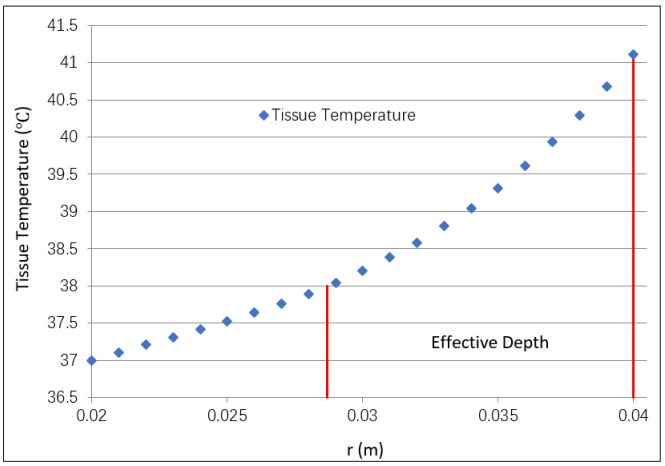

Figure 10: Effective Hyperthermia Depth for Case 2

Case 3

For Case 3, the skin-surface temperature was 39.5 °C and the core temperature remained at 37 °C. Using the same procedure as in the previous cases, the tissue-temperature profile beneath the skin was obtained:

$$T = 4.005 \ln r + 54.241 - 6758.836r^2 + 140095.327r^3$$

Fig.11 shows the resulting temperature distribution. Applying the established criterion for case 3 determining the effective hyperthermia depth, the depth at which normal tissue reaches the threshold temperature is 9.0 mm in this case (see Fig. 11).

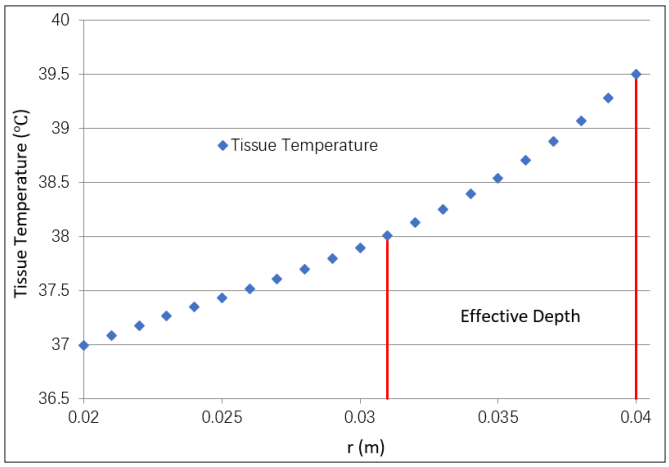

Figure 11: Effective Hyperthermia Depth for Case 3

Through the analysis of the three typical cases, the effective depth of hyperthermia was determined. These cases serve as examples of the analysis procedure; in practice, any skin-surface temperature meeting the hyperthermia threshold can be evaluated using the model to determine the corresponding effective depth.

Skin Temperature Distribution under Different Outdoor Thermal Environment

Because this study considers outdoor thermal conditions as the external source of heating for superficial tumor hyperthermia, the feasibility of the approach depends strongly on the weather. To understand how skin temperature varies across different outdoor environments, multiple measurement sessions were conducted. Fig.12 presents the distribution of skin-surface temperatures recorded across these sessions. As shown in Fig. 12, average skin temperature varied widely in response to changing outdoor conditions. Over a longer observation period, some days provided temperatures that exceeded the threshold needed for mild hyperthermia, while others did not. The horizontal yellow line in Fig. 12 marks the critical temperature threshold: values above this line indicate that skin temperature meets the minimum requirement for hyperthermia, whereas values below it do not. In one-word, outdoor thermal conditions can provide the necessary temperature for superficial hyperthermia, but such conditions are not available every day. The measurements in Fig. 12 illustrate that, under suitable weather, outdoor environments may offer a convenient and low-cost source of heat for this purpose.

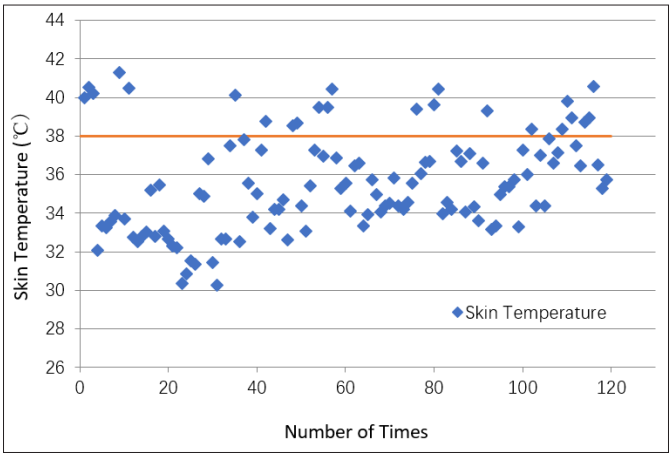

Figure 12: Different Skin Temperatures in Different Outdoor Thermal Environment

To examine how skin temperature responds to outdoor conditions, two key environmental variables, air temperature and solar radiation, were selected for further analysis. Fig.13 illustrates the relationship between skin temperature and air temperature. A positive correlation is observed ($R^2 = 0.458$), indicating that air temperature has a meaningful influence on skin-surface temperature. Fig.14 shows the relationship between skin temperature and solar radiation. Here, the positive correlation is stronger ($R^2 = 0.668$), suggesting that solar radiation plays an even more significant role in determining skin temperature. In both figures, skin temperature follows the general trend of the corresponding environmental variable, but solar radiation appears to be the dominant factor.

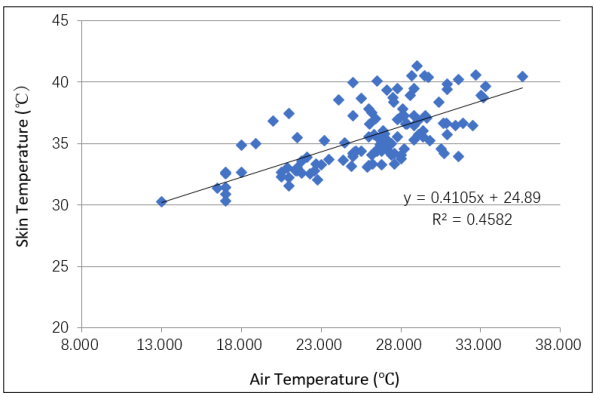

Figure 13: Relationship between Skin Temperature and Air Temperature

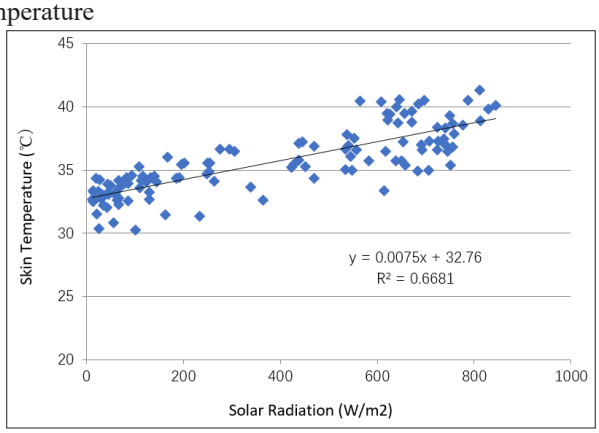

Figure 14: Relationship between Skin Temperature and Solar Radiation

Discussions

Hyperthermia has gained increasing clinical attention in recent years. Many hospitals in China have incorporated hyperthermia as an adjunctive treatment for tumors, and several studies report therapeutic benefits. Research and clinical observations indicate that heat-based interventions can suppress tumor growth by damaging tumor cells, disrupting tumor-associated vasculature, and activating immune responses. Experimental work has investigated the effects of controlled thermal environments on tumor development. For example, studies using BALB/c 4T1 breast-tumor mouse models found that continuous exposure to an elevated thermal environment significantly slowed tumor growth. After 21 days of heating, histopathological analysis showed extensive tumor-cell necrosis, suggesting a clear cytotoxic effect. At the same time, tumors in the heated group also showed reduced lactic acid and ATP concentrations compared with controls. In addition, other studies examining cervical Caski tumor cells reported that hyperthermia inhibited cell proliferation, increased apoptosis and necrosis, induced S-phase arrest, and reduced PCNA expression. In addition, changes in Smac/DIABLO and caspase-3 expression at both mRNA and protein levels also depended on the hyperthermia temperature and duration. Collectively, these findings suggest that temperature has a marked influence on tumor-cell proliferation, apoptosis, and related molecular pathways. In clinical practice, hyperthermia protocols vary according to tumor location. Superficial tumors, including various skin tumors such as squamous cell carcinoma, adenocarcinoma, and melanoma, typically require intratumoral temperatures of 39-45 °C, with skin-surface temperatures maintained between 39-43 °C and not exceeding 45 °C. Treatment sessions generally last 30-60 minutes and may extend to 90 minutes when necessary. These temperatures are commonly achieved using dedicated hyperthermia devices such as the BSD2000 hyperthermia machine, We2102-A and We2102-I microwave systems, which are designed to elevate and maintain tissue temperature within the therapeutic range. Given that the essential goal of hyperthermia is to raise tumor temperature to a defined threshold, this study considered whether natural thermal exposure might also contribute to this process. Thus, in addition to temperature elevation through clinical devices, it is reasonable to ask whether natural conditions could also produce a comparable rise in tissue temperature. Therefore, this study examines whether natural thermal exposure in outdoor environments could contribute to the recovery process for superficial skin tumors. Outdoor thermal conditions are shaped by multiple factors, including global climate change, surface-material characteristics, population activity, and the seasonal movement of the sun, all of which create continuous variation throughout the year. Although outdoor conditions do not consistently meet the temperature requirements for hyperthermia, suitable thermal environments do occur during certain periods, particularly in late spring, summer, and early autumn, when skin-surface temperatures may approach the mild hyperthermia range. This study suggests that, under certain conditions, natural outdoor thermal environments may reach temperatures comparable to mild superficial hyperthermia. In summary, hyperthermia is an established approach in tumor treatment, and tumor-cell behavior is influenced by the surrounding thermal environment. The findings indicate that superficial skin tumors may at times reach temperatures within the mild hyperthermia range under specific outdoor conditions. For patients who have already completed anti-tumor therapy, such conditions may offer an additional source of thermal exposure that could help support recovery. This possibility may contribute to improving the five-year survival rate of patients with superficial skin tumors [47-50].

Conclusions

The paper established a new mathematical model to estimate tissue temperatures at different depths using skin-surface temperature as a boundary condition. An analytical solution to the bio-heat transfer equation was derived, allowing tissue temperatures beneath the skin to be calculated. By combining these temperature distributions with the critical thresholds for hyperthermia, the effective treatment depth for superficial tumors can be determined. The analysis shows that this effective depth is directly influenced by the skin-surface temperature. The results show that skin-surface temperature varies across different outdoor thermal conditions. Under certain conditions, skin temperatures may reach levels comparable to mild hyperthermia, suggesting that specific outdoor environments have the potential to achieve temperatures relevant to superficial tumor hyperthermia. The findings also suggest that, when used appropriately and with awareness of the effective heating depth, selected outdoor thermal environments could offer a potential avenue of thermal exposure for individuals with superficial tumors. This represents a new conceptual direction, presented here for the first time, and warrants further investigation by other researchers. The main conclusions are as follows:

- A new bio-heat transfer model was developed, and its analytical solution produced reasonable tissue-temperature distributions, offering a simpler alternative to complex numerical methods;
- The effective tissue depth for tumor hyperthermia was identified by combining the critical hyperthermia temperature with the temperature distributions generated from the model;
- The analysis of skin temperature and key outdoor thermal parameters indicates that the effective hyperthermia depth is influenced by outdoor environmental conditions.

Acknowledgements

The authors would like to thank the National Natural Science Foundation of China (52578110); Chongqing Natural Science Foundation Innovation and Development Joint Funds Program (CSTB2025NSCQ-LZX0002) for their financial support, without which this research paper would not have been possible.

Declaration of Competing Interest

The authors declare that they have no financial interests or personal relationships that could have appeared to influence the work reported in this paper.

References

1. Chunxiao Zhang, Yang Yang, Le Yu (2025) Assessing urban surface thermal environment and heat health risk in Chinese cities: A twenty-year study. Urban Clim 59: 102304.
2. Fanzhuo Zhou, Zhaojun Wang, Yuxin Yang, Chang Liu, Jia Zhao (2025) Field study on effect of large temperature steps on thermal comfort and physiological response in severe cold climate. Build Environ 268: 112338.
3. Shanshan Wang, Lan Wang, Haoru Wu, Xiquan Chen, Wenwen Xu, et al. (2025) Impact of age on children's outdoor thermal sensation in a hot and humid climate. Build Environ 271: 112652.
4. Junmeng Lyu, Yuxin Yang, Dayi Lai, Li Lan, Zhiwei Lian (2024) Exploring the correlation and synchronicity between environmental factors and occupant thermal response in dynamic outdoor cabin environments. Build Environ 261: 111727.
5. Wenjie Song, Fangliang Zhong, John Kaiser Calautit, Jiaxiang Li (2025) Exploring the role of skin temperature in thermal sensation and thermal comfort: A comprehensive review. EBE 6: 762-781.
6. Xiaowen Su, Ongun Berk Kazanci, Bjarne W Olesen, Liangliang Sun, Yanping Yuan (2025) A novel method of calculating mean skin temperature with high thermal sensitivity for thermal sensation evaluation. Energy Build 340: 115809.
7. Guoqing Yu, Runnan Lu, Xing Lv, Shuang Feng (2025) Local thermal sensation model with local skin temperature and local skin heat flux in a personalized heating microenvironment. Energy Build 332: 115429.
8. Mingxuan Luo, Fei Guo, Haiquan Tang, Ruiqi Ming, Li Huang, et al. (2025) A systematic review of the influence of physiological factors on outdoor thermal comfort. HSS 1: 27-40.
9. Huihui Zhao, Genyu Xu, Yurong Shi, Yongchao Zhai, Lihua Zhao, et al. (2024) Evaluation of pedestrian thermal comfort from a whole-trip perspective: An outdoor empirical study. SCS 115: 105872.
10. Julian Anders, Sebastian Schubert, Bjorn Maronga, Mohamed Salim (2025) Simplifying heat stress assessment: Evaluating meteorological variables as Single indicators of outdoor thermal comfort in urban environments. Build Environ 274: 112658.
11. Jiaqi Zhao, Rui Wang, Yeyu Wu, Chaoyi Zhao, Yun Qi, et al. (2024) From characteristics to practical applications of skin temperature in thermal comfort research - A comprehensive review. Build Environ 262: 111820.
12. Wonseok Oh, Ryozo Ooka, Junta Nakano, Hideki Kikumoto, Osamu Ogawa (2020) Evaluation of mist-spraying environment on thermal sensations, thermal environment, and skin temperature under different operation modes. Build Environ 168: 106484.
13. Chuangkang Yang, Ruizi Zhang, Hiroaki Kanayama, Daisuke Sato, Keiichiro Taniguchi, et al. (2025) Hybrid personalized thermal comfort model based on wrist skin temperature. Build Environ 268: 11232.
14. Vishakha G Bodele, Swati N Lade, Diksha S Undirwade, Milind Janrao Umekar, Sushil S Burle, et al. (2025) Transforming oncology with carbon quantum dots: Synthesis, properties and therapeutic potential. Next Nanotechnology 7: 100181.
15. Cuihua Gu, Jinzhong Zhang, Wenhua Gao, Jisong Wang, Kun Mou, et al. (2025) Advances and applications of hyperthermia in tumor therapy: Mechanisms, techniques, and clinical integration. International Communications in Heat and Mass Transfer 164: 108895.
16. P Wust, B Hildebrandt, G Sreenivasa, Rau B, Gellermann J, et al. (2002) Hyperthermia in combined treatment of cancer. Lancet Oncol 3: 487-497.
17. MM Paulides, H Dobsicek Trefna, S Curto, DB Rodrigues (2020) Recent technological advancements in radiofrequency- and microwave-mediated hyperthermia for enhancing drug delivery. Adv Drug Deliv Rev 163: 3-18.
18. Kanwal Ahmed, Syed Faisal Zaidi, Mati-ur-Rehman, Rehman R, Kondo T (2020) Hyperthermia and protein homeostasis: Cytoprotection and cell death. J Therm Biol 91: 102615.
19. Shoshana Burke, Menachem Hanani (2021) The actions of hyperthermia on the autonomic nervous system: Central and peripheral mechanisms and clinical implications. Auton Neurosci 168: 4-13.
20. Michael Dunne, Maximilian Regenold, Allen C (2020) Hyperthermia can alter tumor physiology and improve chemo- and radio-therapy efficacy. Adv Drug Deliv Rev 163: 98-124.
21. Weiwei Zhu, Siwei Pan, Jiaqing Zhang, Jingli Xu, Ruolan

Zhang, et al. (2024) The role of hyperthermia in the treatment of tumor. Crit Rev Oncol Hematol 204: 104541.

22. Marloes IJff, Johannes Crezee, Arlene L Oei, Stalpers LJA, Westerveld H (2022) The role of hyperthermia in the treatment of locally advanced cervical cancer: a comprehensive review. Int J Gynecol Cancer 32: 288-296.
23. Mehdi Jaymand (2024) Hydrogel-based drug delivery systems for synergistic chemo/hyperthermia therapy of cancer: A comprehensive review. Journal DDST 95: 105581.
24. M Teresa, Yaiza Castillo, Lozano Lorca M, Morales Martínez A, Arrabal Polo MÁ, et al. (2024) Efficacy of conduction hyperthermia in the treatment of non-muscle invasive bladder cancer: A systematic review. Urol Oncol 42: 251-265.
25. Beik J, Abed Z, Ghoreishi FS, Hosseini Nami S, Mehrzadi S, et al. (2016) Nanotechnology in hyperthermia cancer therapy: From fundamental principles to advanced applications. J Control Release 235: 205-221.
26. Bert Hildebrandt, Peter Wust, Ahlers O, Dieing A, Sreenivasa G, et al. (2002) The cellular and molecular basis of hyperthermia. Crit Rev Oncol Hematol 43: 33-56.
27. Ackerman SJ, Rein AL, Blute M, Beusterien K, Sullivan EM, et al. (2000) Cost effectiveness of microwave thermotherapy in patients with benign prostatic hyperplasia: part I methods. Urology 56: 972-979.
28. Paul Cherukuri, Evan S Glazer, Curley SA (2010) Targeted hyperthermia using metal nanoparticles. Adv Drug Deliv Rev 62: 339-345.
29. G Lassche, J Crezee, CML Van Herpen (2019) Whole-body hyperthermia in combination with systemic therapy in advanced solid malignancies. Crit Rev Oncol Hematol 139: 67-74.
30. Caitlin Tydings, Karun V Sharma, Ae Rang Kim, Pavel S Yarmolenko (2020) Emerging hyperthermia applications for pediatric oncology. Adv Drug Deliv Rev 163-167.
31. Datta NR, Ordóñez SG, Gaipl US, Paulides MM, Crezee H, et al. (2015) Local hyperthermia combined with radiotherapy and-/or chemotherapy: Recent advances and promises for the future. Cancer Treat Rev 41: 742-753.
32. Oei AL, Kok HP, Oei SB, Horsman MR, Stalpers LJA, et al. (2020) Molecular and biological rationale of hyperthermia as radio- and chemosensitizer. Adv Drug Deliv Rev 163: 84-97.
33. Ping Yuan (2009) Numerical analysis of an equivalent heat transfer coefficient in a porous model for simulating a biological tissue in a hyperthermia therapy. Int J Heat Mass Transf 52: 1734-1740.
34. Saqib Mubarak, MA Khanday, Ahsan Ul Haq (2020) Variational finite element approach to study heat transfer in the biological tissues of premature infants. J Therm Biol 92: 102669.
35. Ozen S, Helhel S, Cerezci O (2008) Heat analysis of biological tissue exposed to microwave by using thermal wave model of bio-heat transfer (TWMBT). Burns 34: 45-49.
36. Yuwen Zhang (2009) Generalized dual-phase lag bioheat equations based on nonequilibrium heat transfer in living biological tissues. Int J Heat Mass Transf 52: 4829-4834.
37. NO Moraga, F Corvalán, M Escudey, A Arias, CE Zambra (2009) Unsteady 2D coupled heat and mass transfer in porous media with biological and chemical heat generations. Int J Heat Mass Transf 52: 5841-5848.
38. Xingmou Liu, Lei Li, Yan Gu, Wei Tang, Ammad Jadoon, et al. (2022) Numerical investigation on losses and heat-transfer characteristics of Magnetic-heat therapy in deep biological tissue based on magnetothermal gel with medium frequency vortex. JMMM 557: 169469.
39. MM Tung, M Trujillo, JA López Molina, MJ Rivera, EJ Berjano (2009) Modeling the heating of biological tissue based on the hyperbolic heat transfer equation. Mathematical and Computer Modelling 50: 665-672.
40. Said Camilleri J, Farrugia L, Curto S, Rodrigues DB, Farina L, et al. (2022) Review of Thermal and Physiological Properties of Human Breast Tissue. Sensors 22: 3894.
41. Pankaj Kishore, Sumit Kumar, Vipul M Patel (2022) Conjugate heat transfer analysis of laser-irradiated cylindrical-shaped biological tissue embedded with the optical inhomogeneity. Int Commun Heat Mass Transfer 137: 106302.
42. Yundong Tang, Yuesheng Wang, Rodolfo CC Flesch, Tao Jin (2023) Influence of different heat transfer models on therapeutic temperature prediction and heat-induced damage during magnetic hyperthermia. J Therm Biol 118: 103747.
43. Teerapot Wessapan, Phadungsak Rattanadecho (2016) Flow and heat transfer in biological tissue due to electromagnetic near-field exposure effects. Int Commun Heat Mass Transfer 97: 174-184.
44. Luo Qing (2019) Heat Transfer, Chongqing University Press, China. J T B 26-29.
45. Lin Qing yuan, Yang Hong qin, Xie Shu sen, Chen Shu qiang, Ye Zheng (2007) Finite element analysis for temperature distribution of normal breast. Acta Laser Biology Sinica 906-928.
46. Zhu Guangming (2026) Study of Bio-Heat Transfer for Some Practical Applications, PhD Dissertation, Huazhong University of Science and Technology, China. JTB 35-42.
47. Tang Y, Yu H, Zhong X, Zhang K, Mao H, et al. (2025) Understanding local thermal comfort and physiological responses in older people under uniform thermal environments. Physiol Behav 292: 114832.
48. Dayi Lai, Xiaojie Zhou, Qingyan Chen (2017) Measurements and predictions of the skin temperature of human subjects on outdoor environment. Energy Build 151: 476-486.
49. Ziqi Hu, Zhihao Wan, Zhaoying Wang, Huan Zhang, Sujie Liu, et al. (2025) Machine learning modeling of indoor thermal sensation under solar radiation considering skin temperatures. Build Environ 275: 112822.
50. B Erdmann, J Lang, M Seebass (1998) Optimization of temperature distributions for regional hyperthermia based on a nonlinear heat transfer model. Ann N Y Acad Sci 858: 36-46.